Journal of Fluorine Chemistry 181 (2016) 30–35

Contents lists available at ScienceDirect

Journal of Fluorine Chemistry

journal homepage: www.elsevier.com/locate/fluor

One-step synthesis of high-purity Li_2BeF_4 molten salt

Guoqiang Zong, Zhen-Hua Cui, Xiao-Gang Sun, Ji-Chang Xiao *

Key Laboratory of Organofluorine Chemistry, Shanghai Institute of Organic Chemistry, Chinese Academy of Sciences, 345 Lingling Road, Shanghai 200032, China

ARTICLE INFO

Article history:
Received 1 June 2015
Received in revised form 26 September 2015
Accepted 28 October 2015
Available online 10 November 2015

Keywords:
FLiBe molten salt
One-step synthesis
$(NH_4)_2BeF_4$
Recrystallization

ABSTRACT

$(NH_4)_2BeF_4$ was synthesized and purified by recrystallization to remove sulfate ions before being used as the main raw material to prepare Li_2BeF_4 molten salt. $(NH_4)_2BeF_4$ was heated and melted with LiF at high temperature to produce Li_2BeF_4 molten salt without separate BeF_2 preparation by pyrolysis. The obtained salt has a melting point of 458–460 °C and an oxygen content below 500 ppm. The main impure metal ion and anion concentrations are less than 10 ppm and 80 ppm, respectively. This is a convenient, efficient and economical preparative method for high-purity Li_2BeF_4 molten salt.

1. Introduction

Li_2BeF_4 (FLiBe) molten salt is applied mainly as a heat-transfer medium in nuclear reactors, solar thermal power generation and high-energy batteries. Because of its excellent physical and chemical properties, especially its low absorption and activation neutron characteristics, it is known as "the neutron-transparent fluoride" and is the first choice as molten salt and primary coolant in nuclear reactors [1,2]. FLiBe molten salt of high purity is required in nuclear reactors, because its physical and chemical properties, such as melting point, viscosity, radiation stability and fuel salt dissolution ability, depend largely on FLiBe molten salt purity. For example, oxygen in molten salt usually reacts slowly with nuclear fuel to form a paste or results in UO_2 and ThO_2 deposition in the reactor. This decreases nuclear fuel solubility, and results in local loop overheating and other serious consequences. In addition, there is a limited number of elements with high neutron absorption cross-section and strong corrosive oxygen ions in FLiBe molten salt [3,4].

High purity BeF_2 is one of the main raw materials used to prepare FLiBe molten salt. However, it is unavoidable that the prepared BeF_2 contains sulfate ions, because sulfuric acid leaching of beryllium is an indispensable process during the production of BeF_2. Sulfate ions are corrosive and the main carriers of oxygen in molten salt, and need to be removed in FLiBe molten salt preparation. Most methods developed and tested at Oak Ridge National Laboratory for the removal of sulfate ions and oxide impurities from fluoride salts are based on high-temperature treatment with H_2 and HF gas mixtures [5–8]. However, this requires considerable expenditure on special equipment, monitoring systems and personnel safety since HF is extremely corrosive, H_2 is flammable and explosive, and the reaction time is more than 70 h. For the preparation of small batches of salts, this process is not justified economically. Therefore, a new preparation method is essential to obtain high-quality FLiBe molten salt under mild, laboratory conditions.

We used a "source control" strategy to remove sulfate ions in $(NH_4)_2BeF_4$, which is the precursor of BeF_2, by repeated recrystallization. $(NH_4)_2BeF_4$ and LiF were heated and melted in a molar ratio of 33.3:66.7. High-purity FLiBe molten salt was synthesized at high temperature by a one-step method. This method eliminates the need for a separate process to prepare BeF_2 and for a long time to treat molten salt with H_2–HF. During $(NH_4)_2BeF_4$ decomposition, HF is generated and is used to reduce the oxygen content in the FLiBe molten salt. This method has many advantages, such as mild reaction conditions, simple operation, low equipment requirements, good economy and low risk (Scheme 1).

2. Results and discussion

2.1. Recrystallization of $(NH_4)_2BeF_4$

In crystal form, $(NH_4)_2BeF_4$ exists as a three-dimensional network composed of tetrahedral BeF_4^{2-} linked to one another,

* Corresponding author. Tel.: +86 21 5492 5340; fax: +86 21 6416 6128.
E-mail address: jchxiao@sioc.ac.cn (J.-C. Xiao).

http://dx.doi.org/10.1016/j.jfluchem.2015.10.017
0022-1139/

$$(NH_4)_2BeF_4 + LiF \xrightarrow[-\ NH_3,\ -\ HF]{\text{Neat, }\triangle} Li_2BeF_4$$

Scheme 1. One-step Li_2BeF_4 synthesis.

and the electric charge, shape and crystal size of the BeF_4^{2-} are very similar to SO_4^{2-} [9]. This suggests that BeF_4^{2-} and SO_4^{2-} possess crystallographic isomorphic properties and cause crystal mixture precipitation of BeF_4^{2-} and SO_4^{2-} during recrystallization. Recrystallization conditions need to be optimized to obtain high crystallinity and high purity $(NH_4)_2BeF_4$.

$(NH_4)_2BeF_4$ is soluble in water, and insoluble in solvents such as ethanol, methanol, acetone and ethyl acetate. We added 17% ($v_{solvents}$:v_{water} = 1:5) non-aqueous solvents into water to form mixed solvents, and $(NH_4)_2BeF_4$ recrystallization was carried out in these mixed solvents. To study the impact of non-aqueous solvents on $(NH_4)_2BeF_4$ yield and SO_4^{2-} removal efficiency, 75 °C was chosen as the initial crystallization temperature, the cooling rate was set to 4 °C h^{-1} and the final temperature was 5 °C, with the results shown in Table 1. All experiments were repeated three times, and the results of SO_4^{2-}content are presented as mean ± standard deviation (SD). When these nonelectrolytes are added to the salt-water system, the water molecules prefer to be surrounded by nonelectrolyte molecules rather than electrolyte ions, which leads to a decrease in proportion of "free water". The links between salt and water molecules therefore weaken, salts are transported far from the water molecules and gather together, and this results in over-saturation and precipitation [10,11]. If we consider the yield of $(NH_4)_2BeF_4$ and the removal efficiency of SO_4^{2-}, an ethanol–water mixed solvent was chosen as the recrystallization mixed solvent. Compared with a single water solvent, the $(NH_4)_2BeF_4$ solubility is lower in the ethanol–water mixed solvent, and this type of solvent can yield stable $(NH_4)_2BeF_4$ crystal shapes.

During recrystallization, the cooling rate of saturated solution was found to be crucial to the product crystal size and purity. Different cooling rates were tested to study their influence on impurity removal efficiency. Determination the content of sulfate ion in $(NH_4)_2BeF_4$ by ion chromatography (IC). It can be seen from Fig. 1 that the SO_4^{2-} content in prepared $(NH_4)_2BeF_4$ decreases significantly with decrease in cooling rate. The $(NH_4)_2BeF_4$ crystal size increases and becomes more regular at a slow cooling rate (Fig. 2). The crystals prepared at lower cooling rate (<4 °C h^{-1}) were rod-like and columnar with low impurity content. If the cooling rate is too rapid (>8 °C h^{-1}), many small crystals that contain large amounts of impurities form. The crystals are small acicular particles. Because the rate of cooling is rapid, solution suddenly enters the unstable region, and causes explosive nucleation. As a result, impurities (such as SO_4^{2-}) are trapped in the crystals.

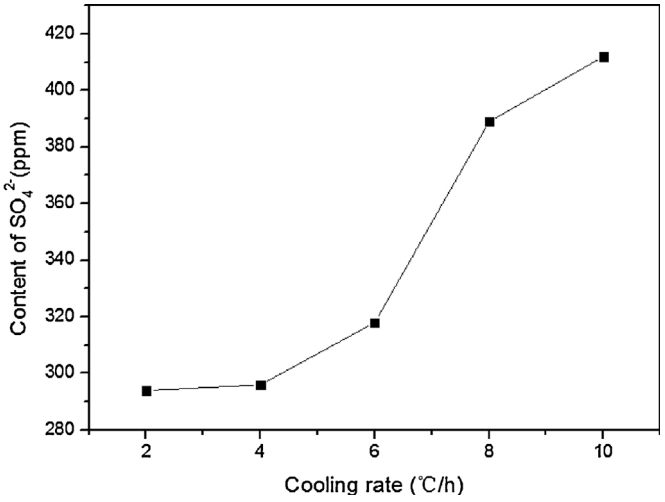

Fig. 1. The cooling rate dependence of the content of SO_4^{2-} in $(NH_4)_2BeF_4$ after recrystallization using ethanol–water mixed solvent. Determination the content of sulfate ion in $(NH_4)_2BeF_4$ by ion chromatography.

Based on these factors, $(NH_4)_2BeF_4$ recrystallization was carried out in a 5:1 water:ethanol solution at an initial recrystallization temperature of 75 °C, a terminal temperature of 5 °C and a cooling rate of 4 °C h^{-1}. The product was purified by two recrystallizations under the same conditions. The final S and SO_4^{2-} contents were 17 ppm and 58 ppm, respectively. The content of other impurities was less than 50 ppm (Table 2). The X-ray diffraction (XRD) pattern of $(NH_4)_2BeF_4$ is shown in Fig. 3 and can be indexed in the orthorhombic crystal system. Values for $(NH_4)_2BeF_4$ are similar to those of the corresponding $(NH_4)_2BeF_4$ [JCPDS Card 01-084-0142, a_0 = 7.65, b_0 = 5.93, c_0 = 10.46]. Using high-purity $(NH_4)_2BeF_4$ as raw material, a single crystal of $(NH_4)_2BeF_4$ was grown from aqueous solution by slow evaporation at room temperature [12,13]. The crystal data and number of reflections are summarized in Table 3. The powder XRD patterns and crystal data show that no detectable impurities were present in the samples, which indicates that the products were single phase.

Table 1
Purification results of $(NH_4)_2BeF_4$ by the recrystallization method with different solvents. The results of SO_4^{2-}content are presented as mean ± standard deviation (SD).

	Content of SO_4^{2-} (SD) (ppm)	Solubility (g)	Yield (%)
Raw material	1279	–	–
Water	408 (3)	47.12	35
Ethanol–water mixed solvent	318 (2)	45.52	38
Methanol–water mixed solvent	334 (3)	40.51	43
Acetone–water mixed solvent	385 (5)	51.88	43
Ethyl acetate–water mixed solvent	383 (1)	45.07	28

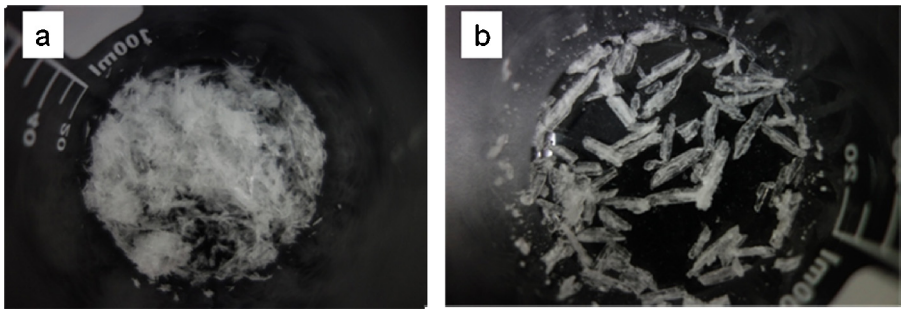

Fig. 2. The appearance of $(NH_4)_2BeF_4$ after recrystallization using ethanol–water mixed solvent with different cooling rate (cooling rate >8 °C h^{-1} (a) and <4 °C h^{-1} (b)).

Table 2
Results (ppm) for impurity elements and SO_4^{2-} determination in $(NH_4)_2BeF_4$ before and after recrystallization in a 5:1 water:ethanol solution by ICP-OES and IC analysis.

Impurities	B	Na	Mg	Si	P	S	Fe	SO_4^{2-}
Raw material	6	26	11	41	7	456	4	1279
Primary recrystallization	2	8	10	41	–	135	–	318
Secondary recrystallization	1	–	7	39	–	17	–	58

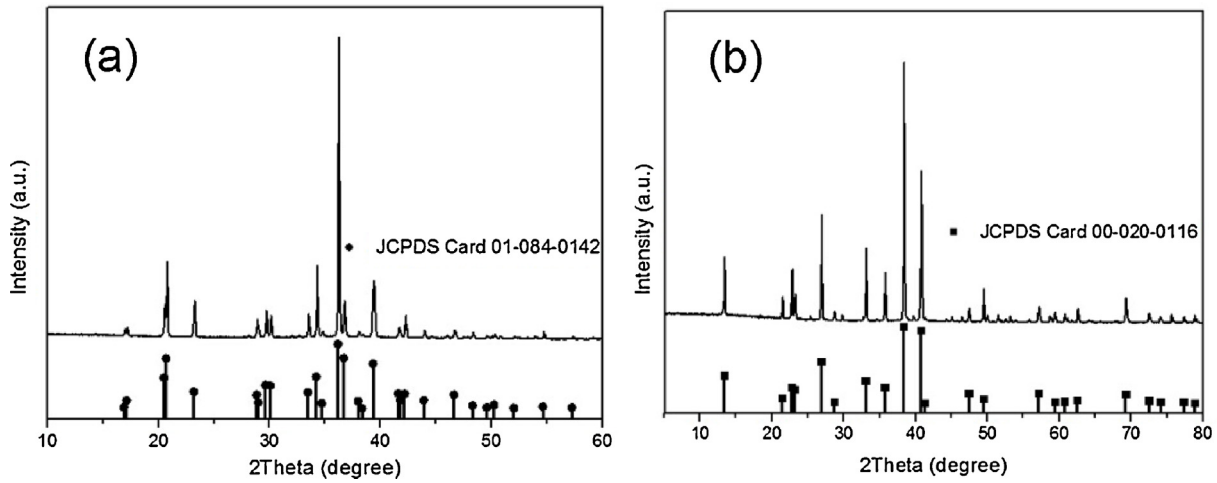

Fig. 3. X-Ray diffraction (XRD) pattern of $(NH_4)_2BeF_4$ after two recrystallizations (a) and Li_2BeF_4 with melting temperature at 650 °C for 3 h (b).

$(NH_4)_2BeF_4$ (24%) remained in the filtrate, which came from suction filtration during recrystallization. The filtrate was collected and mixed with 1.5 times the volume of absolute ethyl alcohol, and a white flocculent precipitate formed. After standing for 5 h, the precipitates were collected by suction filtration and dried at 120 °C in vacuum to recover 85–90% of the material. The reclaimed $(NH_4)_2BeF_4$ can be used as raw material for recrystallization, and increases the economic efficiency.

2.2. Effect of heating rate on oxygen content of FLiBe

The differential scanning calorimetry–thermogravimetric analysis (DSC–TGA) result for the secondary recrystallization crystal particle of $(NH_4)_2BeF_4$ is shown in Fig. 4. $(NH_4)_2BeF_4$ began to decompose at ~200 °C, and the reaction was completed almost entirely at ~450 °C. The final weight (%) is 38.5% at 650 °C, which is consistant with the final theoretical weight of 38.8% based on the decompositon reaction. With the further increase of temperature, there is a small amount of volatile fluoride. For FLiBe molten salt preparation, the mixture of $(NH_4)_2BeF_4$ and LiF (molar ratio 33.3:66.7) was melted by gradient heating in a vacuum induction melting furnace. A selection of heating rates was crucial to the oxygen content of the molten salt in the temperature range of $(NH_4)_2BeF_4$ decomposition. If the heating rate were too rapid during this period, $(NH_4)_2BeF_4$ would decompose rapidly, and HF produced by decomposition could not react fully with oxygenated chemicals and would result in a high oxygen content in the molten salt. Control of $(NH_4)_2BeF_4$ decomposition rate would be useful for slow HF generation. The gas would be able to mix fully with the molten salt, react completely with the oxygenated chemicals and remove the oxygen-containing material.

After complete decomposition, the mixture was heated to and maintained at 650 °C for 3 h to prepare FLiBe molten salt. The final oxygen contents in molten salt for an increase in temperature from 200 °C to 450 °C are shown in Table 4. When the heating rate was

Table 3
Crystal data of $(NH_4)_2BeF_4$ and Li_2BeF_4.

	$(NH_4)_2BeF_4$	Li_2BeF_4
Space group	Pnma	*R*3̄
Crystal system	Orthorhombic	Trigonal
Formula unit per Unit cell (*Z*)	4	18
Unit cell dimensions	$a = 7.6269(17)$ Å $\alpha = 90°$ $b = 5.9083(13)$ Å $\beta = 90°$. $c = 10.428(2)$ Å $\gamma = 90°$	$a = 13.282(2)$ Å $\alpha = 90°$ $b = 13.282$ Å $\beta = 90°$ $c = 8.8934(14)$ Å $\gamma = 120°$
Volume	469.91(18) Å^3	1358.6(5) Å^3
Density (calculated)	1.712 Mg/m^3	2.176 Mg/m^3
Independent reflections	485 [R(int) = 0.0697]	705 [R(int) = 0.0235]
Final R indices [$I > 2$sigma(I)]	$R1 = 0.0440$, $wR2 = 0.1103$	$R1 = 0.0172$, $wR2 = 0.0527$
R indices (all data)	$R1 = 0.0449$, $wR2 = 0.1114$	$R1 = 0.0195$, $wR2 = 0.0546$

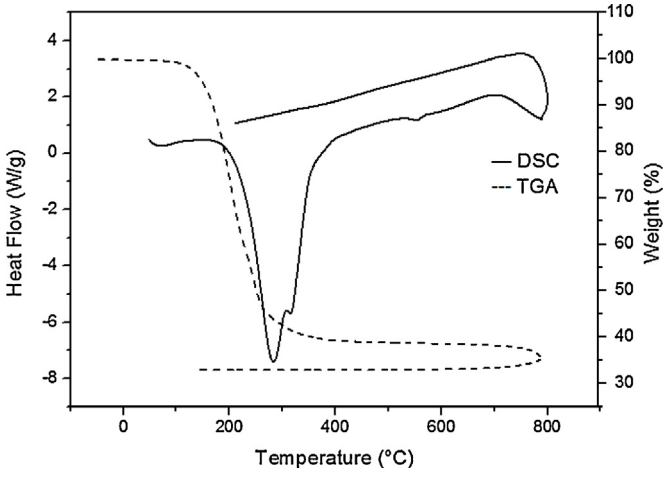

Fig. 4. DSC–TGA of $(NH_4)_2BeF_4$.

Table 4
Effect of temperature raising procedure on oxygen content of molten salt.

Time over which the temperature is increased from 200 to 450 °C (h)	Heating rate (°C min^{-1})	Oxygen content (ppm)
0.5	8.4	1650
1	4.2	1200
2	2.1	978
3	1.4	460
4	1.0	458

8.4 °C min^{-1}, the oxygen content in the molten salt was as high as 1650 ppm. The oxygen content decreased with decrease in heating rate and because there was little difference in oxygen content between a heating rate of 1.4 °C min^{-1} and 1.0 °C min^{-1}, the former was selected as the final heating rate.

2.3. Effect of melting temperature and time on FLiBe quality

After $(NH_4)_2BeF_4$ had decomposed from 200 °C to 450 °C, mixtures were heated to different temperatures (500 °C, 600 °C, 650 °C and 750 °C) to maintain melting. The preservation time was set for 3 h at the different melting temperature. The results show that the fluoride salts reluster and look like sinter if the smelting temperature is too low. When the melting temperature reached 650 °C, the product was white, homogeneous and contained glossy crystals (Fig. 5). An analysis of the DSC curve of the molten salt sample (Fig. 6), showed that molten salt prepared under this temperature condition could form typical endothermic and exothermic melting peaks. If the melting temperature were too high (>750 °C), the molten salt would volatilize and lose mass, which would lead to a ratio change of salt mixtures during the process. When the reaction time was set at 2 h, 3 h or 4 h, the melting time had little effect on molten salt quality for the same melting temperature (650 °C). An appropriate melting temperature was 650 °C and reaction time was 3 h.

Fig. 5. FLiBe molten salt sample.

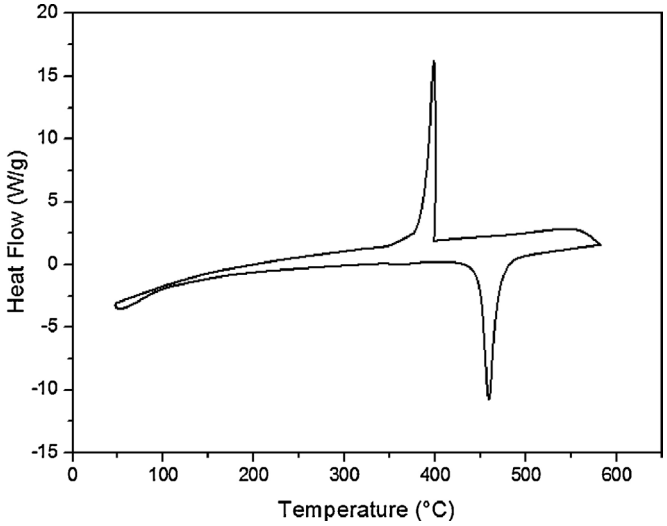

Fig. 6. DSC of FLiBe molten salt.

Table 5
Results (ppm) for metal impurities determination in FLiBe using the ICP–OES determination.

Metal impurity	Cr	Mn	Fe	Ni	Mo	Ti	Al	Co	W
1	<5	<5	<5	5.3	<5	<5	5.7	<5	<5
2	<5	<5	5.4	<5	<5	5.7	5.9	<5	5.2
3	<5	6.2	5.4	<5	5.3	6.1	<5	5.3	5.4
4	6.5	<5	5.2	5.3	5.3	5.9	6.3	<5	5.4
5	<5	<5	5.2	5.7	<5	<5	6.1	<5	<5
6	<5	5.6	<5	<5	5.6	<5	<5	<5	<5
7	5.4	<5	<5	6.8	<5	<5	<5	5.3	5.6

The melting point of prepared FLiBe molten salt was 458–460 °C. The metal impurities and neutron poison content in the molten salt prepared by the new method were all lower than 10 ppm and the oxygen content was lower than 500 ppm (Tables 5–7). Compared with the traditional H_2–HF method [5,6], the one-step method also reduces the oxygen content and metal impurities would not be introduced into molten salt by the graphite crucible during the new preparation process. The XRD pattern of Li_2BeF_4 is shown in Fig. 3. The value for Li_2BeF_4 is similar to that of the corresponding Li_2BeF_4 [JCPDS Card 00-020-0116, $a_0 = 13.29$, $c_0 = 8.91$]. Single crystals of Li_2BeF_4 grew by slow cooling of the melt salt mixtures, which agreed with the experimental results in literature [14]. The crystal data and number of reflections are summarized in Table 3. The powder XRD pattern and crystal data indicate that the products were crystallographically pure.

Table 6
Results (ppm) for anion impurities determination in FLiBe using the IC determination method.

Anion impurity	Cl^-	NO_2^-	NO_3^-	PO_4^{3-}	SO_4^{2-}
1	38	<5	11	22	56
2	16	<5	8.7	15	72
3	14	<5	<5	21	43
4	22	<5	<5	12	56
5	36	<5	8.9	27	66
6	23	<5	<5	16	78
7	32	<5	<5	18	67

Table 7
Content of oxygen and melting point analytical data in FLiBe using inert gas fusion-infrared absorption method and TGA measurement.

Entry	1	2	3	4	5	6	7
Oxygen content (ppm)	467	420	398	489	451	412	444
Melting point (°C)	458	458	458	460	460	459	458

Sheet 1. Temperature rise by gradient style when preparing FLiBe molten salt.

3. Conclusion

A new one-step synthesis method was developed to prepare high-purity FLiBe molten salt by smelting a mixture of LiF and purified $(NH_4)_2BeF_4$ under high-temperature conditions. $(NH_4)_2BeF_4$ decomposes at high temperature to form BeF_2 and release HF. BeF_2 was a raw material used to prepare the molten salt. HF can be used as fluorinating agent to remove oxygen from the molten salt and oxide impurities. This method is more efficient, simple to operate, convenient, safe and of benefit in industrial production.

4. Experimental

4.1. Purification of ammonium fluoroberyllate ($(NH_4)_2BeF_4$)

$(NH_4)_2BeF_4$ was prepared according to literature [9]. $Be(OH)_2$ was reacted with hydrofluoric acid and ammonia in aqueous solution. The resultant precipitates were washed and dried at 120 °C. The as-prepared $(NH_4)_2BeF_4$ powders were dissolved in a recrystallization solvent. The water bath was heated and stirred for 3 h until the solution became transparent. The saturated solution was then cooled slowly and a large amount of white precipitate was formed. The precipitate was collected by suction filtration, washed several times with absolute ethanol and then dried at 120 °C. The product could be recrystallized several times according to need. The dried $(NH_4)_2BeF_4$ was characterized by ion chromatography (IC), inductively-coupled plasma spectrometer (ICP) and TGA.

4.2. Preparation of FLiBe molten salt

LiF (99.9%) and $(NH_4)_2BeF_4$ were kept at 400 °C and 120 °C in a vacuum drying oven, respectively, for 4 h to remove water before being used. To prepare FLiBe molten salt, molar ratios of the initial mixtures were 33.3 $(NH_4)_2BeF_4$:66.7 LiF. The typical synthesis procedure is as follows: $(NH_4)_2BeF_4$ (121.09 g) and LiF (51.88 g) were mixed and added to a graphite crucible. The crucible was sealed in a vacuum induction melting furnace, and the furnace chamber pressure was kept at 10 Pa for 1 h to remove traces of water from fluoride salts under high vacuum conditions. The furnace chamber was then recharged with high-purity nitrogen to permit a minor positive pressure and the mixture was melted according to a preset temperature program (Sheet 1). After completion of melting, salts were transferred to an airtight storage tank and cooled naturally to room temperature. The FLiBe molten salt was ground to a fine power on a special device in a dry glove box and then characterized by IC, ICP, TGA and trance oxygen analyzer.

A double-layer structure was used in the vacuum induction furnace. Internal circulating water was used to form a cooling wall. The cooling wall surface was treated using Teflon spray to achieve anti-corrosion properties. The highly toxic release of HF and NH_3 combined with NH_4F condensed on the cooling wall. Vaporization products could then be removed easily from the FLiBe molten salt system to avoid molten salt pollution.

4.3. Characterization

IC analysis was performed using a Thermo SCIENTIFIC IC-1100 chromatograph. Anion concentrations were determined using a system fitted with a 2 mm ASRS column. The mobile phase is composed of 9 mM Na_2CO_3 gradient elution at a 0.25 mL min^{-1} flowrate and 25 μL injection volume. ICP–OES analysis was by SPECTRO ARCOS spectrometer. Typically, a molten salt sample was dissolved in 2% HNO_3 solution. The operating conditions were: forward power 1.43 kW, argon gas flow rate 12.00 L m^{-1} (plasma), 0.9 L min^{-1} (auxiliary), 0.78 L min^{-1} (nebulizer) and spectral purity (99.99%) argon gas. TGA measurements were conducted using a TA SDT-Q600 thermogravimetric system. Samples (~10 mg) were sealed hermetically in an aluminum pan, heated to 800 °C at 20 °C min^{-1} and held for 3 min and then cooled to room temperature at the same rate. Phase constitutions were identified by powder XRD using an X'Pert Pro diffractometer with Cu*K*α radiation operated at 40 kV and 40 mA. Oxygen content analysis was carried out using a Leco O836 meter. Fluoride is corrosive and will volatilize easily at high temperature and damage the detection system, so a halogen trap assembly was installed after the cracking furnace to eliminate pollution by fluoride vapor [15]. X-ray Crystallography. Suitable single crystals of $(NH_4)_2BeF_4$ and Li_2BeF_4 were mounted under nitrogen atmosphere on a glass fiber, and data collection was performed on a Bruker APEX2 diffractometer with graphite-monochromated Mo *K*α radiation (λ = 0.71073 Å). The SMART program package was used to determine the unit cell parameters. The absorption correction was applied using SADABS. The structures were solved by direct methods and refined on F^2 by full-matrix least-squares techniques with anisotropic thermal parameters for non-hydrogen atoms. Hydrogen atoms were placed at calculated positions and were included in the structure calculation. All calculations were carried out using the SHELXL-97 program. The software used is listed in Ref. [16].

Acknowledgements

This work was financially supported by the Strategic Leading Science and Technology Projects of Chinese Academy of Sciences (XDA02020105, XDA02020106), the National Natural Science Foundation of China (21172240, 21421002, 21472222), National Basic Research Program of China (2015CB931900, 2012CBA01200).

Appendix A. Supplementary data

Supplementary material related to this article can be found, in the online version, at http://dx.doi.org/10.1016/j.jfluchem.2015.10.017.

References

[1] D.-K. Sze, M.E. Sawan, E.T. Cheng, Fusion Technol. 39 (2001) 789–792.
[2] A. Suzuki, T. Terai, S. Tanaka, J. Nucl. Mater. 258–263 (1998) 519–524.
[3] S. Delpech, C. Cabet, C. Slima, G.S. Picard, Mater. Today 13 (2010) 34–41.
[4] J. Uhlir, J. Nucl. Mater. 360 (2007) 6–11.
[5] G. Smolik, R. Pawelko, Y. Morimoto, K. Okuno, R. Anderl, D. Petti, T. Terai, J. Nucl. Mater. 329–333 (2004) 1322–1326.
[6] M. Hara, Y. Hatano, M.F. Simpson, G.R. Smolik, J.P. Sharp, Y. Oya, K. Okuno, M. Nishikawa, T. Terai, S. Tanaka, R.A. Anderl, D.A. Petti, D.K. Sze, Fusion Eng. Des. 81 (2006) 561–566.
[7] R.A. Anderl, S. Fukada, G.R. Smolik, R.J. Pawelko, S.T. Schuetz, J.P. Sharpe, B.J. Merrill, D.A. Petti, H. Nishimura, T. Terai, S. Tanaka, J. Nucl. Mater. 329–333 (2004) 1327–1331.
[8] J.H. Shaffer, Preparation of and handling of salt mixtures for the molten salt reactor experiment, in: ORNL-4616, January 1971, January 1971.

[9] В.И. Spicin, The Chemical Technology and Metallurgy Beryllium, USSR, Moscow, 1960.
[10] S. Mosseri, Z.B. Alfassi, Sep. Sci. Technol. 18 (1983) 165–175.
[11] D.A. Weingaertner, S. Lynn, D.N. Hanson, Ind. Eng. Chem. Res. 30 (1991) 490–501.
[12] A. Onodera, Y. Shiozaki, Ferroelectrics 19 (1978) 23–24.
[13] A. Onodera, Y. Shiozaki, J. Phys. Soc. Jpn. 46 (1979) 157–166.
[14] J.H. Burns, E.K. Gordon, Acta Crystallogr 20 (1966) 135–138.
[15] G.-Q. Zong, B. Chen, M. Gao, J.-C. Xiao, Chin. J. Inogr. Anal. Chem. 5 (2015) 45–48.
[16] (a) G.M. Sheldrick, SADABS, An Empirical Absorption Correction Program for Area Detector Data, University of Göttingen, Göttingen, Germany, 1996;
(b) G.M. Sheldrick, SHELXS-97 and SHELXL-97, University of Göttingen, Göttingen, Germany, 1997;
(c) Bruker AXS Inc., SMART Version 5.628, Bruker AXS Inc., Madison, WI, 2002;
(d) Bruker AXS Inc., SAINT+ Version 6.22a, Bruker AXS Inc., Madison, WI, 2002;
(e) Bruker AXS Inc., SHELXTL NT/2000, Version 6.1, Bruker AXS Inc., Madison, WI, 2002.